Available online at www.sciencedirect.com
ScienceDirect
Journal of Chromatography B, 859 (2007) 16–23
JOURNAL OF CHROMATOGRAPHY B
www.elsevier.com/locate/chromb

Mechanistic analysis on the effects of salt concentration and pH on protein adsorption onto a mixed-mode adsorbent with cation ligand

Dong Gao [a,b], Dong-Qiang Lin [a], Shan-Jing Yao [a,*]

[a] *Department of Chemical and Biochemical Engineering, Zhejiang University, Hangzhou 310027, PR China*
[b] *Institute of Modern Separation Science, Key Laboratory of Separation Science in Shaanxi Province, Northwest University, Xi'an 710069, PR China*

Received 23 April 2007; accepted 30 August 2007
Available online 19 September 2007

Abstract

Streamline Direct HST is a new kind of mixed-mode adsorbent with cation exchange ligand, especially developed for the expanded bed adsorption process, which can capture target protein directly from the moderate ionic strength feedstock without the need of dilution or other additives. In this study, the isotherm adsorption behaviors and the isocratic retention factors of bovine serum albumin (BSA) on Streamline Direct HST were measured, and the corresponding adsorption mechanisms were also described. The results indicated that Streamline Direct HST shows the typical property of salt-independent adsorption and the maximum binding capacity of BSA occurs near the isoelectric point of BSA. When there are some amounts of electrostatic repulsion protein–adsorbent interactions, the multilayer adsorption could be found, and high salt concentration does not favor the adsorption of protein. A patch-controlled adsorption process and an oriented adsorption model are proposed for describing the adsorption behaviors under electrostatic repulsion condition.

Keywords: Mixed-mode chromatography; Streamline Direct HST; Multilayer adsorption; Patch-controlled adsorption; Oriented adsorption

1. Introduction

Mixed-mode interaction chromatography is a special chromatographic technology that combines more than one mode of adsorption, most commonly hydrophobic and ion exchange adsorptions [1]. With the multifunctional chromatographic matrix, such as silica gel with silanol groups [2], mixed-mode chromatography can often provide multiple types of interactions. The target molecule can be adsorbed either at low conductivity in the ion-exchange mode or at high conductivity in the hydrophobic interaction mode, and the elution can be achieved at the moderate conductivity. Burton et al. [3] reported a kind of mixed-mode adsorbent based on the cellulose matrix combining hydrophobic and electrostatic interactions with high ligand density for separation of chymosin, which showed a specific property of salt-independent adsorption. The charged groups of the ligand at low ionic strength perform the ion-exchange adsorption of target protein. As the ionic strength increases the aromatic ring of ligand allows the hydrophobic interaction to target protein for salt-tolerant adsorption. Therefore, high binding capacities can usually be achieved at the moderate conductivity (10–30 mS/cm). The desorption of the target protein can be induced with the electrostatic charge repulsion and accomplished by changing the pH of mobile phase across the isoelectric point of protein. This technique is especially suitable for expanded bed adsorption (EBA) to capture target protein directly from the moderate ionic strength feedstock without the need of dilution or other additives [4,5]. It was found that the literature on mixed-mode chromatography has been largely focused on the applications [3,5,6]. Hamilton et al. [6] reported the direct product sequestration of an extracellular protease from a microbial batch culture with the mixed-mode EBA process, which had the potential to significantly cut costs and process time. Lu et al. [5] used the mixed-mode EBA adsorbent of Fastline PRO to capture nattokinase directly from *Bacillus subtilis* fermentation broth. The purification factor could reach 12.3, which demonstrated the advantage of mixed-mode EBA in enzyme separation.

Streamline Direct HST, a new kind of mixed-mode adsorbent with cation exchange ligand, was developed for the EBA process

* Corresponding author. Tel.: +86 571 87951982; fax: +86 571 87951015.
E-mail address: yaosj@zju.edu.cn (S.-J. Yao).

1570-0232/$ – see front matter © 2007 Elsevier B.V. All rights reserved.
doi:10.1016/j.jchromb.2007.08.044

by GE Healthcare. The ligand is a multimodal functional group, which can bind proteins with a high capacity even in high ionic strength feedstocks. Li et al. [7] reported the protein adsorption and desorption with Streamline Direct HST. Charoenrat et al. [8] reported the equilibrium capacity and the dissociation of β-glucosidase with Streamline Direct HST. However, no detailed adsorption behaviors under different conditions and the corresponding mechanisms with this new adsorbent have been reported. The limitation of the understanding of adsorption mechanisms certainly impedes the applications of new mixed-mode adsorbent Streamline Direct HST.

The aim of this work is to investigate the protein adsorption behaviors with Streamline Direct HST under different salt concentration and pH. Bovine serum albumin (BSA) will be used as the model protein for adsorption. The adsorption mechanism under different conditions would be discussed in detail, too.

2. Materials and methods

2.1. Materials

Bovine serum albumin (BSA) (A-7030), with a MW of 67 kDa and a theoretical p*I* of 4.9, was obtained from Sigma (Milwaukee, WI, USA). Streamline Direct HST was a kind gift from GE Healthcare (Uppsala, Sweden). The ligand structure of Streamline Direct HST adsorbent is shown in Fig. 1, and some properties given by the manufacturer are listed in Table 1. Other reagents were of analytical reagent grade and purchased from local suppliers.

2.2. Adsorption isotherms

For the adsorption equilibrium experiments, the drained adsorbents of different mass were added to 15 ml BSA solution in the appropriate buffer containing different NaCl concentrations. The adsorption experiments were conducted at 25 °C for 10 h in a shaking incubator. After adsorption equilibrium, the solid-phase was separated, and the supernatant was analyzed for protein concentration. The adsorbed mass of protein was calculated from the mass balance. The following buffers were used at a concentration of 0.02 M: phosphate–citric acid, pH 2.4 and 3.0; citric acid–citrate, pH 4.0–6.0; phosphate, pH 7.0.

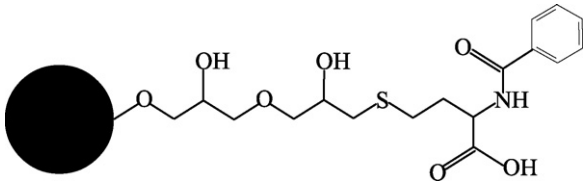

Fig. 1. Structure of the mixed-mode ligand in the Streamline Direct HST adsorbent.

Table 1
Some properties of Streamline Direct HST adsorbent

Matrix structure	Macroporous cross-linked 4% agarose containing stainless steel materials
Functional group	Multi-modal weak cation exchanger
Type of exchanger	High salt-tolerant
Total ionic capacity[a]	0.07–0.09 mmol H^+/ml medium
Particle form	Spherical, 80–165 μm
Mean particle size	135 μm
Mean particle density	1.8 g/ml

[a] The parameter is from the packed bed adsorbent Capto MMC with the same ligand as Streamline Direct HST from GE healthcare.

2.3. Retention experiments

All retention experiments were conducted with the ÄKTA Explorer 100 chromatographic system from Amersham Biosciences (Uppsala, Sweden). 1 cm × 10 cm column with about 4 ml adsorbent was used. The flow rate was set at 1.0 ml/min. Following the equilibration of column with the appropriate buffer, 0.5 ml protein samples were injected into the column. The fluid effluent was monitored at 280 nm for peak detection. The column void volume was obtained by measuring the protein retention volume under pH 10.0 and 2 M sodium chloride. The retention factor (k') was calculated using the equation as following

$$k' = \frac{V_R - V_0}{V_0} \quad (1)$$

where V_R is the retention volume for the solute corrected by the system delay, and V_0 is the column void volume.

2.4. Measurement of hydrodynamic diameter of protein

The hydrodynamic diameter of BSA was measured by Zetasizer Nano ZS (Malvern Instruments, UK). BSA was dissolved in the appropriate buffer to the concentration of 1 mg/ml. The buffer was filtrated using a 0.22 μm filter. Measurements were carried out in triplicate at 25 °C and the average value was reported. The following buffers were used at a concentration of 0.02 M: phosphate–citric acid, pH 2.4 and 3.0; citric acid–citrate, pH 4.0–6.0; phosphate, pH 7.0; glycine–NaOH, pH 9.0–10.0; carbonate–NaOH, pH 10.5 and 11.0.

3. Results and discussion

3.1. Effect of pH on the BSA adsorption

The adsorption behaviors of BSA on Streamline Direct HST were investigated at different pHs of 0.02 M appropriate buffer (pH 2.4, 3.0, 4.0, 4.4, 5.0 and 5.4) with 0.2 M NaCl. The isotherm adsorption data were shown in Fig. 2. The data were correlated with the Langmuir equation as follows

$$Q = \frac{Q_m C}{K_d + C} \quad (2)$$

where Q is the protein adsorption capacity and C is the protein concentration in the bulk solution. The apparent Langmuir parameters, maximum binding capacity (Q_m) and dissociation coefficient (K_d), were obtained by fitting the experimental data and shown in Fig. 3.

The isoelectric point of BSA is about 4.9. As pH values changes from 5.0 to 2.4, the net positive charges on the surface of

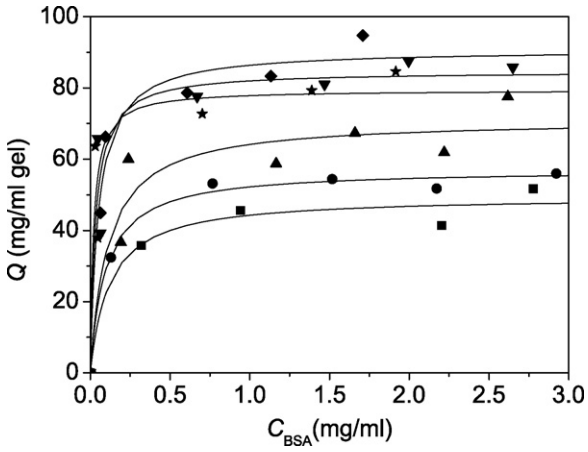

Fig. 2. Effect of pH on the adsorption equilibrium of BSA onto Streamline Direct HST at 25 °C: (■) pH 2.4; (●) pH 3.0; (▲) pH 4.0; (▼) pH 4.4; (♦) pH 5.0; (⋆) pH 5.4. Symbols represent experimental data, and solid lines represent the correlated results with Langmuir equation.

BSA increase obviously, so it seems that the maximum binding capacity (Q_m) should be obtained at pH 2.4. However, as shown in Figs. 2 and 3, the maximum binding capacity could be found around the isoelectric point of the protein. This phenomenon might be contributed by several reasons. The interaction forces between protein molecules and Streamline Direct HST can be classified as the hydrophobic interaction, electrostatic interaction and hydrogen bonding interaction. Hydrogen bonds are formed between hydroxyl–carbonyl or hydroxyl–amide radicals. When the pH value of solution is below 4.0, Streamline Direct HST will show a combination of hydrophobic interaction, hydrogen-bonding interaction and weak electrostatic interaction with BSA. With the decrease of pH the electrostatic attractive interaction between BSA and the adsorbent is obviously decreased due to the reducing numbers of dissociated carboxyl groups on the adsorbent below pH 4.0, which will not favor the electrostatic adsorption of BSA onto Streamline Direct HST. On the other hand, the conformational change of protein could also influence the adsorption process. BSA exists in a compact form between pH 4.3 and 10.5 [9]. The decrease of pH resulted in the transition of BSA conformation from heart-shape (N form) to cigar-shape (F form) at pH 4.5 and the conformation changes were nonreversible when pH < 4.0 [10]. Such transition always involves an expansion of the molecule. Dzhafarov [11] found that the surface area accessible to solvent increased from 39,000 to 70,400 Å^2 during the N–F transition of BSA. In order to verify the analysis mentioned above, the hydrodynamic diameter (D_h) of BSA with the function of pH at constant ionic strength (0.2 M NaCl) was measured. As shown in Fig. 4, the results indicated strongly the same tendency reported by Martenson [12]: when the pH values change from 5.0 to 2.4, the hydrodynamic diameter of BSA increases from about 7.0 to 9.2 nm, and the relative increase of molecular volume is from about 180 to 408 nm^3. It implies that the decrease of the adsorption capacity with the decrease of pH could be considered as a result of the increase of the molecular volume of BSA. Similar results were also reported in the literature [13].

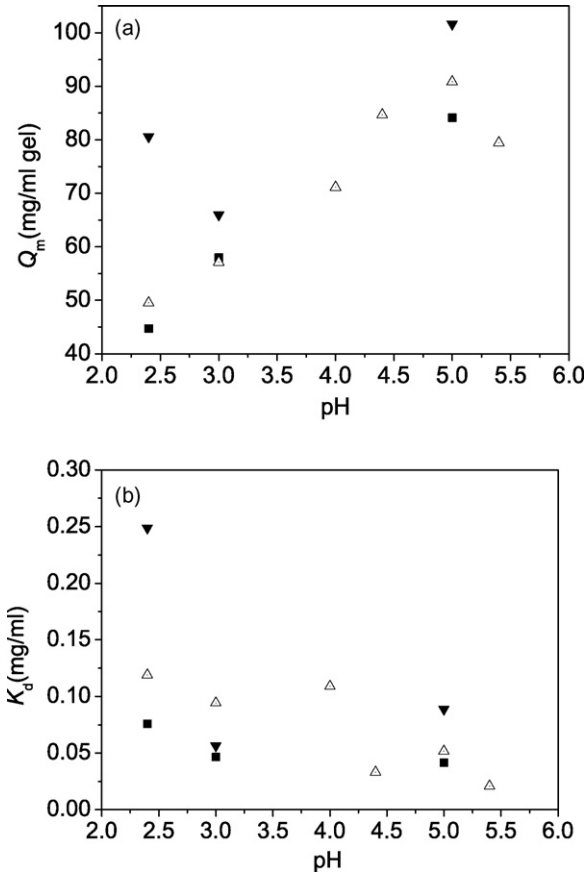

Fig. 3. Effect of pH on the maximum binding capacity Q_m (a) and apparent dissociation coefficient K_d (b) at 25 °C correlated with Langmuir equation: (■) 0.05 M NaCl; (△) 0.20 M NaCl; (▼) 0.50 M NaCl.

3.2. Effect of salt concentration on BSA adsorption

Salt concentration is another important factor relative to mixed-mode adsorption behavior. Fig. 5 shows the isotherm adsorption curves under different salt concentrations with varying pH values. The apparent maximum binding capacity and apparent dissociation coefficient were also shown in Fig. 3. As

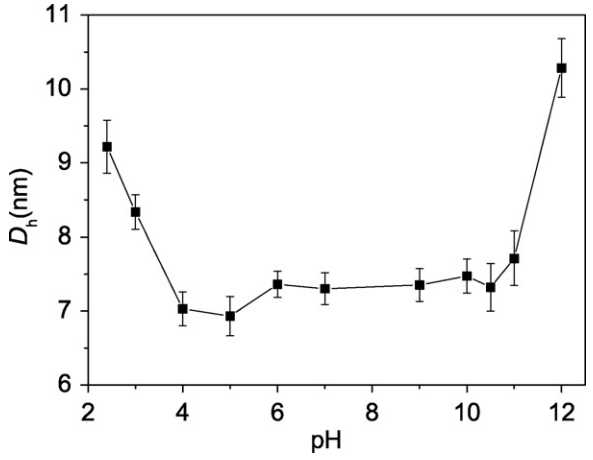

Fig. 4. Variation of hydrodynamic diameter (D_h) with pH at constant ionic strength: 0.02 M buffer plus 0.2 M NaCl.

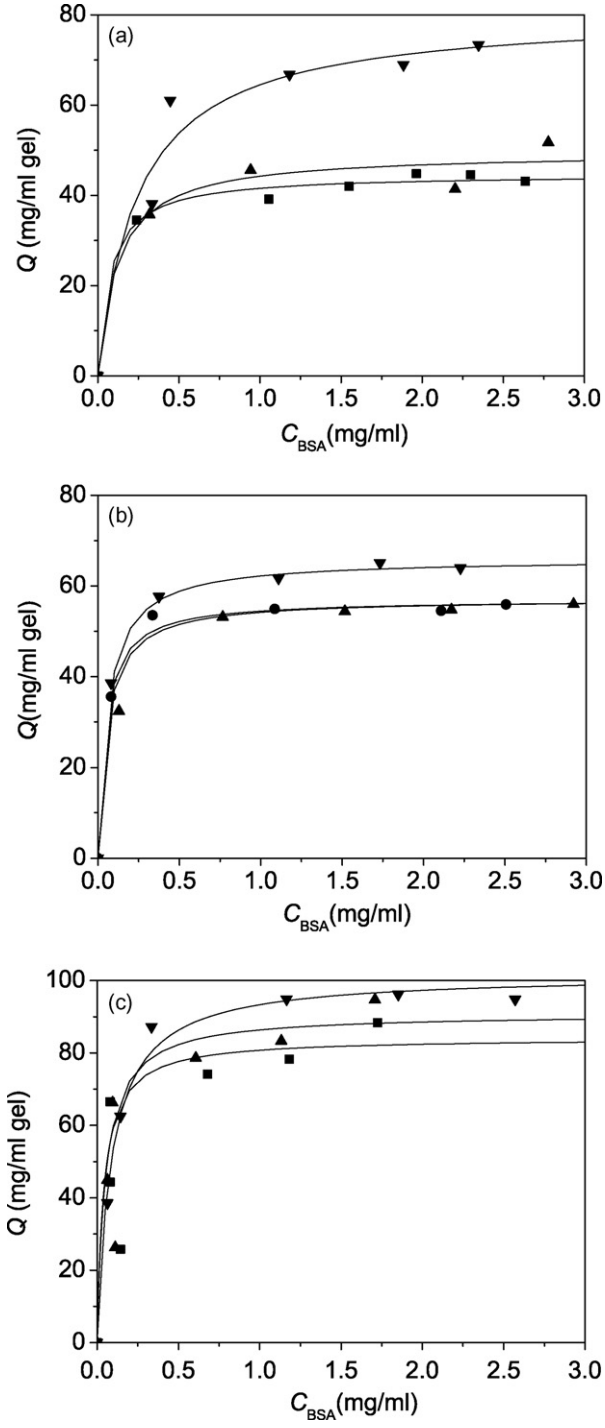

Fig. 5. Effect of salt concentration on the adsorption equilibrium of BSA onto Streamline Direct HST at 25 °C and different pH values: (a) pH 2.4; (b) pH 3.0; (c) pH 5.0. (■) 0.05 M NaCl; (▲) 0.20 M NaCl; (▼) 0.50 M NaCl. Symbols represent experimental data, and solid lines represent the correlated results with Langmuir equation.

mentioned above, when the pH value of solution is below 4.0, the dominant interactions are hydrogen bonding and hydrophobic interactions, which control the protein adsorption. The increasing salt concentrations could reinforce the hydrophobic interaction between protein molecule and adsorbent, resulting in the increase of adsorption capacity. In addition, the molecular

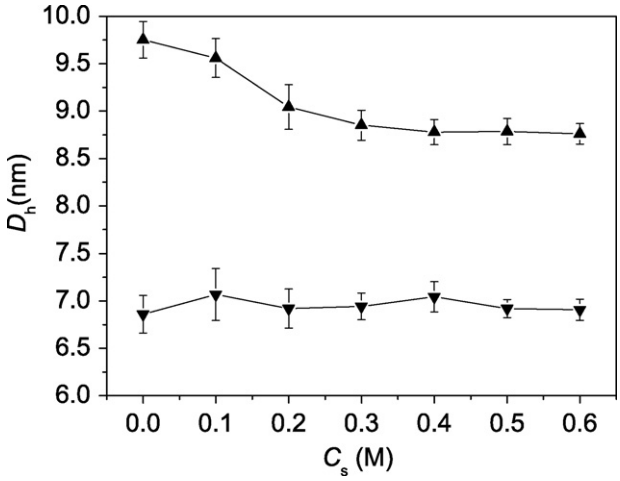

Fig. 6. Variation of hydrodynamic diameter (D_h) with NaCl concentration in 20 mM buffer: (▲) pH 2.4 and (▼) pH 5.0.

volume of BSA changes with the salt concentration in solution. As shown in Fig. 6, when the salt concentration increases from 0 to 0.5 M, the hydrodynamic diameter of BSA decreases from about 9.8 to 8.8 nm in 20 mM citrate buffer at pH 2.4, and the relative decrease of molecular volume is found from 493 to 357 nm^3. At pH 5.0 the molecular size of BSA keeps relatively constant under different salt concentrations. The results are consistent with Martenson's report [12]. Therefore, the decrease in molecular volume with the increasing salt concentration is another factor for the increase of adsorption capacity, and the most significant change of adsorption capacity on salt concentration could be found at pH 2.4, as can be seen from Fig. 5. From Fig. 3b, it is also evident that the apparent dissociation coefficient K_d decreases with increasing pH value and decreasing salt concentration. This behavior suggests that the maximal affinity between protein and adsorbent is around the isoelectric point of BSA and at the low salt concentration.

3.3. Adsorption behaviors under the electrostatic repulsion conditions

When the solution pH value is above the p*I* of BSA (pH > 4.9), the electrostatic repulsion interaction between the apparent negatively charged protein and the dissociated carboxyl groups will occur, and certainly this does not favor the adsorption of protein onto the adsorbent. Fig. 7 shows the isotherm curves under the electrostatic repulsion conditions. Three tendencies can be summarized as follows: the net negatively charged protein molecules may also adsorb onto the negatively charged adsorbent; the adsorption curves might illustrate a multilayer adsorption process; high salt concentration does not favor the adsorption of protein. The adsorption behaviors would be analyzed step by step in the following section.

It is well known that chromatographic behavior is determined by the functional groups located in the contact regions [14]. That is, for the binding of protein onto the adsorbent with ionic ligand, the counter-ions on the adsorbent were displaced by only a fraction of charged amino acid residues on the protein surface.

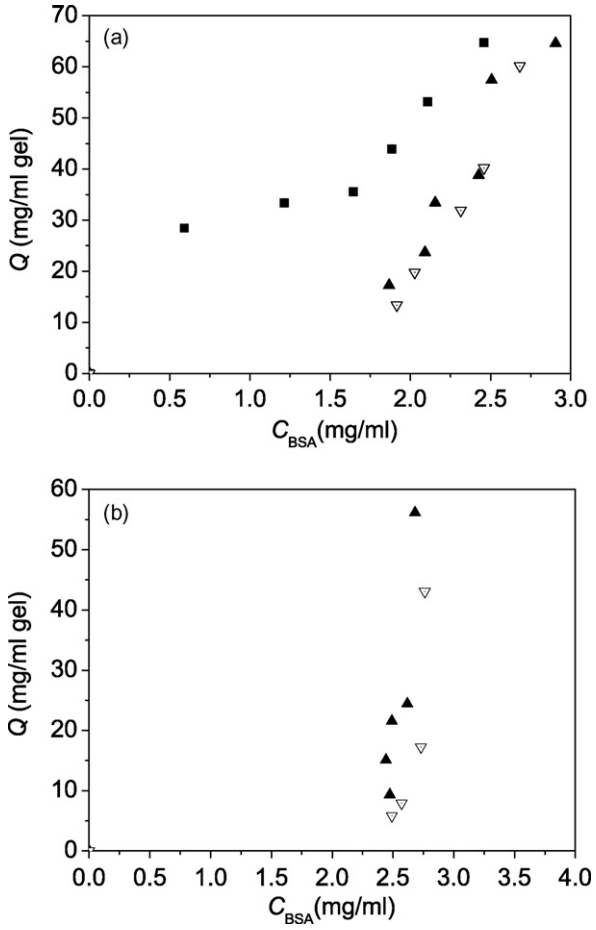

Fig. 7. Effect of salt concentration on the adsorption equilibrium of BSA onto Streamline Direct HST at 25 °C and different pH values: (a) pH 6.0 and (b) pH 7.0. (■) 0.05 M NaCl; (▲) 0.20 M NaCl; (▽) 0.50 M NaCl. Symbols represent experimental data.

The three-dimensional structure of human serum albumin (HSA) was used for the analysis, which is almost identical with that of BSA [10]. The PDB file (ID: 1AO6) containing the molecular structure information of HSA was downloaded from the public resource of Protein Data Bank (PDB) [15]. The Delphi V4.0 program based on the linearized Poisson–Boltzmann equation with a finite difference algorithm was used to calculate the electrostatic potential around protein [16]. The surface potentials distribution and electrostatic potential isocurves of HSA molecule at pH 7.0 could be observed with PyMOL program, and the results are illustrated in Fig. 8. It can be seen that more negative charges are located in the domains I and II whereas positive charges are mainly distributed in the domain III. This asymmetrical charge distribution strongly suggests an oriented *side-on* adsorption site as indicated by the double-headed arrow in Fig. 8d. That is the regions with positive charge groups on the protein surface are more favorable to interact with the negatively charged adsorbent. Therefore, some amount of protein adsorption can also be found under the apparent electrostatic repulsion conditions. This process is similar with the patch-controlled adsorption process of BSA on mixed-mode adsorbent with benzylamine as functional ligand [17].

It can also be seen from Fig. 7, the adsorption isotherm is a typical multilayer adsorption isotherm. The binding capacity increases with the increasing protein concentration. This might be as the result of an oriented adsorption process under the electrostatic repulsion condition as mentioned above. The interaction forces in the protein–adsorbent system can be classified as the protein/adsorbent interaction and the protein/protein interaction, and all interaction forces are the function of pH value and salt concentration. The proposed adsorption mechanism under the electrostatic repulsion conditions is illustrated in Fig. 9. For the initial phase, BSA molecules can orientatively array on the surface of adsorbent during the patch-controlled adsorption process as mentioned above (Fig. 9a). When the protein/adsorbent interaction is the same order of magnitude as the protein/protein interaction under a specific condition, with increasing protein concentration, BSA molecules might adsorb onto the oriented monolayer and form dimers on the surface (Fig. 9b). As illustrated in Figs. 8 and 9, after the orientated *side-on* adsorption of BSA onto the surface of the adsorbent, the region indicated by the single-headed arrow in Fig. 8d would still be accessible to bind a second BSA through the dimer docking sites. Therefore, it could be concluded that the multilayer adsorption of BSA occurs mainly through the protein/protein interactions, and the oriented adsorption should be very important for this process. De Boer and Zwikker [18] attributed the multilayer adsorption to the electrical polarization initiated at a solid polar surface, which induced the dipoles in the first layer of molecules which in turn induced the dipoles in the next layer and so on. This polarized process may be the same as the oriented adsorption process of BSA on Streamline Direct HST under the electrostatic repulsion condition. The similar multilayer adsorption process was also reported in the literature [19].

The ionic strength affects the protein adsorption by adjusting the electrostatic interaction between protein and protein and the hydrophobic interaction and locally electrostatic interaction between protein and adsorbent. With the increase of salt concentration, the hydrophobic interaction would be strengthened, while the electrostatic (attractive and repulsive) interaction would be shielded. Since the multilayer adsorption under the repulsion condition is mainly due to the protein/protein electrostatic interactions, the adsorption capacity will decrease under high salt concentration.

In order to understand better the adsorption tendency under the electrostatic repulsion conditions, the retention behaviors in the chromatographic column were investigated at the corresponding conditions. Fig. 10 shows the plots of the dimensionless retention factor (k') versus salt concentration for BSA at different pHs. The retention factor decreases with the increasing salt concentration. It also indicates that high salt concentration does not favor for the protein adsorption. So it seems that the electrostatic interaction is an important contributor to the protein adsorption for BSA/Streamline Direct HST system under repulsion condition, which is consonant with the results above. Fig. 11 shows the plots of k' versus pH for BSA at different salt concentrations. As can be seen, the retention factor decreases with the increasing pH value. The patch with net positive charge on protein surface is reduced at high pH value, and the repulsion

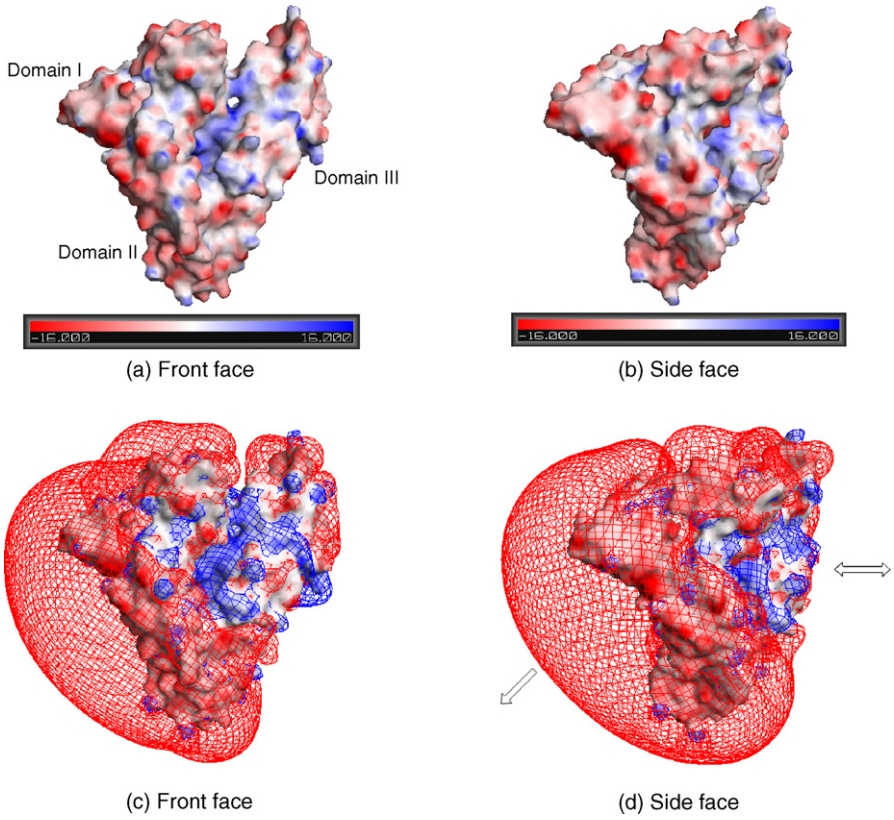

Fig. 8. Surface potentials (a and b) and electrostatic potential isocurves (c and d) (blue: 0.5 kT/e; red: −2.5 kT/e) of HSA at pH 7.0. The double-headed arrow symbolizes the hypothesized *side-on* adsorption site and also indicates a docking site for dimer formation. The single-headed arrow indicates where a second BSA molecule binds into the dimer-docking site and forms a dimer. (For interpretation of the references to color in this figure legend, the reader is referred to the web version of the article.)

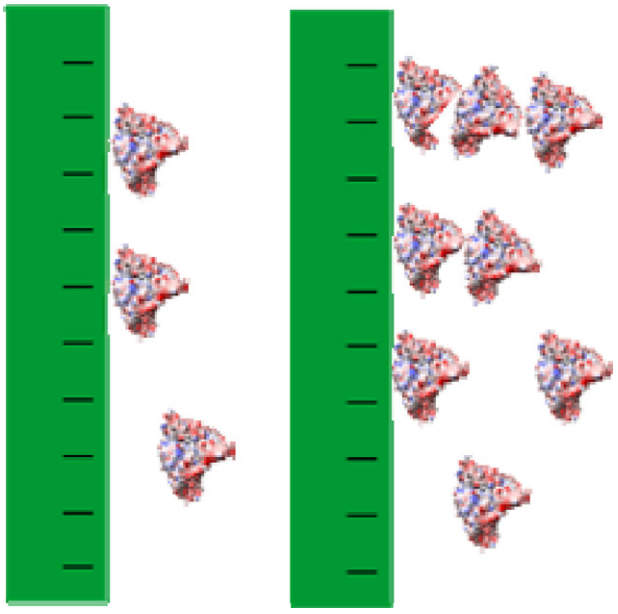

Fig. 9. Proposed adsorption model for BSA on Streamline Direct HST under electrostatic repulsion conditions. During the first adsorption phase (left) the *side-on* monolayer is being formed. Subsequently, in the second adsorption phase (right), dimers are formed through the dimmer-docking site with the protein molecules that are already adsorbed.

interaction between protein and negatively charged adsorbent surface will be strengthened. Elution occurs when the electrostatic repulsive force between the protein and the adsorbent overcomes the hydrophobic interactions. Scopes [20] shows that the pH of the microenvironment of ion exchanger is not the same as that measured in solution. This behavior is known as the Donnan effect that can attract or repulse the protons in the matrices of the adsorbent. In general, the pH in the matrices of a cation

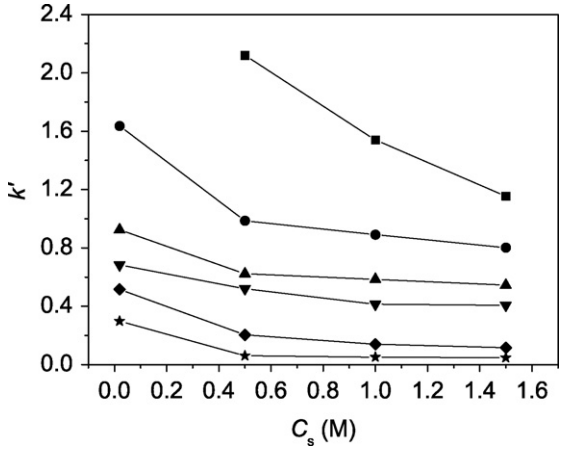

Fig. 10. Plots of k' vs. salt concentration for BSA adsorption on Streamline Direct HST under different pH values: (■) pH 6.0; (●) pH 6.5; (▲) pH 7.0; (▼) pH 8.0; (♦) pH 9.5; (⋆) pH 10.5.

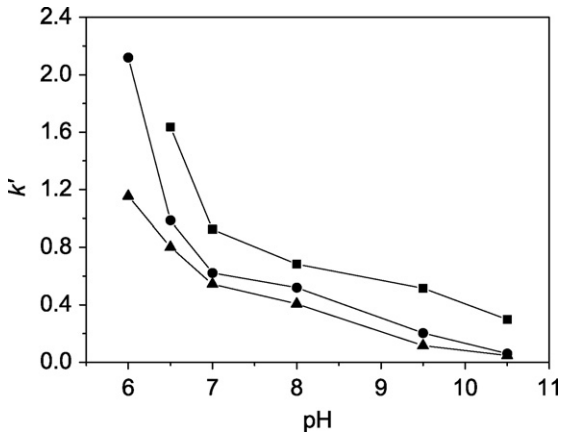

Fig. 11. Plots of k' vs. pH for BSA adsorption on Streamline Direct HST under different NaCl concentrations: (■) 0 M; (●) 0.5 M; (▲) 1.5 M.

exchange adsorbent is one unit lower than that in the solution around. This means that the real pH value in the microenvironment of the adsorbent may be unfavorable for the elution process.

4. Discussion

Streamline Direct HST is a new type of mixed-mode adsorbent for use in EBA process—the technique that captures biomolecules directly from crude, unclarified feedstocks in a single operation unit, without the need of prior clarification. The mixed-mode ligand of Streamline Direct HST is salt-tolerant, so the need to dilute the feedstock to reduce high ionic strength is eliminated. Some mixed-mode ligands were designed for achieving the salt-independent adsorption property [21,22]. However, the recovery was often found to be low due to various intermolecular forces [8,22]. Ligand density may be the first important factor [23]. Typically, the adsorbents of hydrophobic interaction chromatography (HIC) have a relative low ligand density (e.g. 40 μmol/ml) to facilitate the protein recovery by decreasing salt concentration [24]. For higher ligand density, the harsh elution conditions would be necessary for HIC. Mixed-mode chromatographic adsorbents, most commonly containing hydrophobic and ionic groups, have a relative high ligand density (>80 μmol/ml), which is necessary for achieving the salt-independent adsorption property, meanwhile the ionic group is used for the electrostatic repulsion to improve elution process. High ligand density could achieve a high binding capacity, while a stronger desorption condition would be required in the elution process [25]. Streamline Direct HST is a type of cation exchanger with multi-modal functional groups, and has also been found that the recovery was relatively lower than the classical ion exchanger [8,26]. Sometimes the rigorous pH and high salt concentration should be necessary for getting higher elution recovery for target protein.

It was found that the literature has mainly focused on the applications of mixed-mode chromatography [3,5,6], and there is quite few researches dealing with the adsorption mechanism of mixed-mode adsorbent. Li et al. [7] reported the protein adsorption and desorption with Streamline Direct HST. The results showed that the maximum binding capacity occurs near the isoelectric point of BSA, and high salt concentration did not favor the adsorption of protein under the electrostatic repulsion condition. The monolayer adsorption isotherm under the electrostatic repulsion condition was concluded, but the corresponding adsorption mechanisms were not explained. Based on present work mentioned above, the multilayer adsorption isotherm was found and thus the oriented adsorption mechanism was proposed, which can describe the adsorption behavior well.

Charoenrat et al. [8] reported the dissociation of β-glucosidase from Streamline Direct HST. The results showed there was a suitable conductivity required for the maximum dissociation of β-glucosidase from Streamline Direct HST. At low salt concentration the electrostatic change can be applied to dissociation, however, the hydrophobic interaction was increased at high salt concentration while the dissociation ratio decreased and β-glucosidase was bound to the adsorbent again. Based on the present work of BSA adsorption, it seems that different protein could show different adsorption behaviors with Streamline Direct HST, which might be as the result of difference charge distribution on the protein surface. In addition, the present results showed the similar adsorption behavior of BSA on mixed-mode adsorbent with benzylamine as functional ligand [25].

5. Conclusions

In the present work, the effects of liquid phase conditions, pH and salt concentration, on the adsorption behaviors of BSA on mixed-mode adsorbent Streamline Direct HST were studied and the corresponding adsorption mechanisms were also discussed. The results indicate that the maximum binding capacity of BSA on Streamline Direct HST occurs near the isoelectric point of BSA. The conformational change of protein molecule could influence the adsorption process. The adsorption isotherm obeys the Langmuir adsorption equation when the electrostatic attractive interactions exist between protein and adsorbent. When there are some amounts of electrostatic repulsion protein–adsorbent interactions, the multilayer adsorption process could be found, which might be due to the oriented adsorption through the protein/protein interactions. High salt concentration does not favor the protein adsorption under the electrostatic repulsion condition. Different protein results the different adsorption behaviors, and the charge distribution on the protein surface might be main contributor to this phenomenon.

Acknowledgements

The authors are grateful for the financial support of the Hi-tech Research and Development Program of China (863 Program, 2006AA02Z210) and National Natural Science Foundation of China.

References

[1] L.W. Mclaughlin, Chem. Rev. 89 (1989) 309.
[2] L.A. Kennedy, W. Kopaciewicz, F.E. Regnier, J. Chromatogr. 359 (1986) 73.

[3] S.C. Burton, N.W. Haggarty, D.R.K. Harding, Biotechnol. Bioeng. 56 (1997) 45.
[4] S.C. Burton, D.R.K. Harding, J. Biochem. Biophys. Methods 49 (2001) 275.
[5] M.-H. Lu, D.-Q. Lin, Y.-C. Wu, J.-X. Yun, L.-H. Mei, S.-J. Yao, Biotechnol. Bioprocess Eng. 10 (2005) 128.
[6] G.E. Hamilton, F. Leuchau, S.C. Burton, A. Lyddiatt, J. Biotechnol. 79 (2000) 103.
[7] P. Li, G.H. Xiu, V.G. Mata, C.A. Grande, A.E. Rodrigues, Biotechnol. Bioeng. 94 (2006) 1155.
[8] T. Charoenrat, M. Ketudat-Cairns, M. Jahic, S.-O. Enfors, A. Veide, J. Biotechnol. 122 (2006) 86.
[9] C. Tanford, J.G. Buzzell, D.G. Rands, S.A. Swanson, J. Am. Chem. Soc. 77 (1955) 6421.
[10] D.C. Carter, J.X. Ho, Adv. Protein. Chem. 45 (1994) 153.
[11] E.S. Dzhafarov, Mol. Biol. (Mosk) 25 (1991) 1412.
[12] R.E. Martenson, J. Biol. Chem. 253 (1978) 8887.
[13] W. Norde, J. Lyklema, J. Colloid Interface Sci. 66 (1978) 257.
[14] F.E. Regnier, Science 238 (1987) 319.
[15] RCSB Protein Data Bank, http://www.rcsb.org/pdb/.
[16] M.K. Gilson, K.A. Sharp, B. Honig, J. Comput. Chem. 9 (1987) 327.
[17] D. Gao, D.-Q. Lin, S.-J. Yao, Chem. Eng. Sci. 61 (2006) 7260.
[18] J.H. De Boer, C. Zwikker, Z. Phys. Chem. Abt B-3 (1929) 407.
[19] K. Rezwan, L.P. Meier, M. Rezwan, J. Vörös, M. Textor, L.J. Gauckler, Langmuir 20 (2004) 10055.
[20] R.K. Scopes, Protein Purification: Principles and Practice, 2nd ed., Springer-Verlag, New York, 1988, p. 329.
[21] B.-L. Johansson, M. Belew, S. Eriksson, G. Glad, O. Lind, J.-L. Maloisel, N. Norrman, J. Chromatogr. A 1016 (2003) 21.
[22] B.-L. Johansson, M. Belew, S. Eriksson, G. Glad, O. Lind, J.-L. Maloisel, N. Norrman, J. Chromatogr. A 1016 (2003) 35.
[23] S.C. Burton, D.R.K. Harding, J. Chromatogr. A 814 (1998) 71.
[24] J.L. Ochoa, Biochimie 60 (1978) 1.
[25] D. Gao, D.-Q. Lin, S.-J. Yao, J. Chem. Eng. Data 51 (2006) 1205.
[26] P. Li, G.H. Xiu, A.E. Rodrigues, AIChE J. 51 (2005) 2965.